Colloid and Polymer Science (2021) 299:105–116
https://doi.org/10.1007/s00396-020-04773-7

ORIGINAL CONTRIBUTION

Miscibility, morphology, and properties of poly(butylene succinate) /poly(vinyl acetate) blends

Yi Li[1] · Changyu Han[2] · Liguang Xiao[1] · Yancun Yu[2] · Guangbin Zhou[2] · Mingzhi Xu[2]

Received: 9 May 2020 / Revised: 17 September 2020 / Accepted: 20 October 2020 / Published online: 27 October 2020

Abstract

Poly(butylene succinate) (PBS)/poly(vinyl acetate) (PVAc) blends were prepared by melt mixing. The miscibility, morphology, non-isothermal and isothermal crystallization, and rheological and mechanical properties of PBS/PVAc blends were investigated. The blends were a partial miscible two-phase system with PVAc evenly dispersed in the PBS matrix. The incorporation of PVAc accelerated the crystallization rate of PBS due to the heterogeneous nucleation, but decreased the degree of crystallinity. The rheological properties of PBS were greatly improved by the incorporation of PVAc, because of the high viscosity of PVAc in melt state. The most intriguing result was that the stiffness, strength, and toughness could be improved simultaneously by the addition of PVAc. The modulus, breaking strength, and elongation at break of PBS containing 10 wt% PVAc increased by 3.5%, 15.7%, and 43.4%, respectively. The synergetic improvement in the crystallization, rheological, and mechanical properties may be of much importance for widening the application of PBS.

Keywords Poly(butylene succinate) · Poly(vinyl acetate) · Blend · Miscibility

Introduction

With growing environmental concerns worldwide, the manufacture and use of environmentally friendly biodegradable polymers have gradually attracted more attention [1]. Among the family of biodegradable polymers, poly(butylene succinate) (PBS), synthesized by condensation reaction of succinic acid and 1,4-butanediol, is a promising linear aliphatic semi-crystalline polyester [2, 3]. PBS like many other biodegradable polymers has attracted universal attention due to biodegradable properties, melt processability, and potential applications as environmentally friendly polymers for food packaging, and agricultural and marine applications to replace synthetic nonbiodegradable materials [4, 5]. However, practical application of PBS has been limited due to its low mechanical strength and melt strength. Hence, more and more attention was given to the modification of PBS [6].

In order to improve its performance, many research efforts have been extensively studied including incorporation of fillers, copolymerization, and physical blending. During the past few years, many fillers, such as waste silk fibers [7], glass fiber [8], carbon fiber (CF) [9], montmorillonite (MMT) [10], multiwalled carbon nanotube (MWCNT) [11], kenaf fiber (KF) [12], corn starch (CS) [13], and nano-TiO_2 [14] have been used for the preparation of biocomposites with PBS. However, the compatibility between PBS matrix and fillers, coupled with the dispersion of fillers in the PBS matrix, would affect the performance of PBS composites. Copolymerization modification of PBS, including random and block copolymerization, has been extensively studied. The monomers reported to be randomly copolymerized with PBS include tartaric acid [15], hexylene glycol [16], ethylene succinate [17], and diglycolate [18]. In addition, there are many literatures on PBS block copolymers. Li et al. [19] prepared poly(butylene succinate)-b-poly(diethylene glycol succinate) (PDGS) multiblock copolymers by chain-extension reaction and found the incorporation of PDGS segments decreased the melting and crystallization temperatures

✉ Changyu Han
cyhan@ciac.ac.cn

✉ Liguang Xiao
xlg627@163.com

[1] School of Materials Science and Engineering, Jilin Jianzhu University, Changchun 130118, China

[2] Key Laboratory of Polymer Ecomaterials, Changchun Institute of Applied Chemistry, Chinese Academy of Sciences, Changchun 130022, China

of copolymer. The crystallization and tensile properties of multiblock copolymers consisting of poly(ester urethane) (PEU), PBS, and poly(L-lactic acid) (PLLA) depended on the interaction between different component segments [20]. The copolyesters containing PBS and poly(ethylene succinate) (PES) manifested excellent mechanical properties with fracture stress of 61.8 MPa and fracture strain of 1173% [21]. Additionally, poly(ethylene glycol) (PEG) [22, 23], poly(lactic acid) (PLA) [24], and poly(*p*-dioxanone) (PPDO) [25] etc. are used to synthesize copolymers with PBS. Compared with incorporation of fillers and copolymerization, blending with other polymers is a simple and effective method to improve the multiple properties of polymers. As a result, it has received widespread attention from the industry and academia, and various blends of PBS have been extensively and systematically studied. For example, the immiscible PBS/PLA blends were prepared by melt mixing and showed an obvious improvement in the rheological properties [26]. Wang et al. [27] prepared PBS/poly(butylene adipate) (PBA) blends and found that the PBA could act as a diluter, influencing the morphology of PBS. The partially miscible PBS/PES blends were prepared by solution blending and found that the addition of PES affected the crystallization kinetics of PBS [28].

Poly(vinyl acetate) (PVAc) is an amorphous and transparent polymer and usually can be used as paper finishing agent, binder, and adhesive [29]. PVAc has be blended with many biodegradable polymers to form completely miscible blend systems, such as PLA/PVAc [30, 31], poly(ε-caprolactone) (PCL)/PVAc [29], poly(β-hydroxybutyrate) (PHB)/PVAc [32, 33], and poly(ethylene oxide) (PEO)/PVAc [34]. It had been reported that the hydrogen bonds could be formed between α-hydrogens of PVAc and carboxyl groups from PLA or PHB because of their proton-donating and proton-accepting properties. It was this strong interaction that made polymer blends miscible [31, 32]. Thus, such miscibility and interactions resulted in a definite improvement in the mechanical properties and retarded crystallization behaviors of the blends. For example, in the PLA/PVAc blends, both tensile strength and elongation at break increased with the PVAc content until PVAc rose up to 30 wt% and 5 wt%, respectively [30]. In the case of the PCL/PVAc blend, as the PVAc content increased to 10 wt%, the tensile strength increased while elongation at break decreased [29]. These results meant that there was synergism in the blends possibly due to the increased surface tension of the blends caused by the addition of PVAc [29]. In addition, An et al. [32] found that in the PHB/PVAc blends, PVAc reduced the overall non-isothermal crystallization rate of PHB.

However, little investigation on the binary blends of PBS/PVAc has been reported. The important factor determining the performance of the blends is whether the two components are miscible or not. Therefore, firstly, the main purpose of this work was to study the miscibility and phase morphology of PBS/PVAc blends. Then, the effect of the addition of PVAc on the crystallization and rheological and mechanical properties of PBS/PVAc blends was studied by various techniques in detail.

Experimental

Materials

PBS used in this study was provided by Xinjiang Blue Ridge Tunhe Chemical Industry Joint Stock Co., LTD. with a weight-average molecular weight (M_w) of 1.7×10^5 g mol^{-1} and a polydispersity of 1.82. PVAc was provided by Nuoda New Materials Company with an M_w of 1.5×10^5 g mol^{-1} and a polydispersity of 1.54.

Sample preparation

PBS and PVAc were dried in a vacuum oven at 70 °C for 8 h to avoid hydrolytic degradation. The PBS/PVAc blends were melt blended by using a Haake batch intensive mixer (Haake Rheomix 600, Karlsruhe, Germany), of which the temperature was controlled at 150 °C. The screw speed was 60 rpm and compounding time was 7 min. After blending, all samples were compression molded at 150 °C for 3 min to form a 1-mmthick sheet, and cold-pressed at room temperature. PBS and PVAc in the blends were in the following weight ratios 100/0, 90/10, 80/20, 70/30, and 0/100, where the first number represented PBS and the second represented PVAc.

Characterization

Dynamic mechanical analysis

Dynamic mechanical properties (DMA), storage modulus (E'), and loss factor (tan δ) of pure PBS and PBS/PVAc blends were measured as a function of temperature by using a TA instruments' dynamic mechanical analyzer (DMA) Q800 (USA). The blended samples were thin rectangle with dimensions of $20 \times 10 \times 1.0$ mm^3. The measurement was run in tensile mode with a frequency of 1 Hz. The test temperature ranged from – 60 to 100 °C at a constant heating rate of 3 °C min^{-1}.

Scanning electronic microscopy

The phase morphology of PBS/PVAc blends were examined by a field emission SEM (FEI Co., Eindhoven, Netherlands). The PVAc phase was etched in the acetone solution. Then the etched surfaces of blend samples were sputter coated with

gold. After that, sample surfaces were imaged at an accelerated voltage of 10 kV.

Differential scanning calorimetry

A TA Instruments differential scanning calorimetry (DSC) Q20 (USA) was used to determine the crystallization and thermal behaviors of PBS/PVAc blends. The heat flow and temperature scales were calibrated with indium. The samples were weighted (5–8 mg) and crimp sealed in the aluminum pans. All samples were heated to 150 °C at a heating rate of 100 °C min^{-1}. After isothermalizing at 150 °C for 3 min, the molten samples were cooled to – 60 °C at a rate of 10 °C min^{-1} (first cooling). Then the samples were again heated to 150 °C at a heating rate of 10 °C min^{-1} (second heating). The first cooling and the second heating scans of DSC were used to analyze the non-isothermal melt crystallization and the subsequent heating behaviors. For isothermal crystallization, all samples were heated to 140 °C at a rate of 100 °C min^{-1} and kept for 3 min, then cooled to 90 °C at a rate of 45 °C min^{-1}. The samples were held at 90 °C until the crystallization was complete in order to record the time-dependent crystallization process.

Rheological measurements

Rheological properties of PBS/PVAc blends in dynamic flow field were tested by using a rotational rheometer (TA Series AR2000ex, TA Instrument, USA) device with 25-mm parallel plate geometry. The strain value was set to 1.25% to ensure the linearity of viscoelastic response of samples within the test range. The disc-like shape samples with a thickness of 1 mm were heated to 150 °C, and a frequency scans were performed under a nitrogen atmosphere. The frequency sweep range was 0.05–100 rad s^{-1}.

Tensile tests

According to ISO 527-1:2012 standard, the specimens with a gauge length of 20 mm were prepared and used for mechanical properties testing. The measurements were performed on a tensile testing machine (Instron-1121, USA) at room temperature. The cross-head speed was 200 mm min^{-1}.

Results and discussion

Miscibility and phase morphology

In general, the miscible polymer blend systems show only one glass transition temperature (T_g) caused by the homogeneous state of the amorphous region, and in the immiscible blends, there are two T_gs associated with each individual component. Figure 1 displays the dynamic mechanical traces of PBS/PVAc blends with different PVAc contents. The T_g, a measure of polymer chain mobility, can be measured from tan δ peak and are summarized in Table 1. Neat PBS exhibited a single tan δ peak at around – 18.5 °C, and neat PVAc showed a sharp single tan δ peak at around 49.6 °C, corresponding to their glass transition, respectively. For PBS/PVAc blends, there were two glass transitions on the tan δ curves, the higher one corresponded to PVAc phase, and the lower one corresponded to PBS phase, suggesting that PBS/PVAc blends were not thermodynamically miscible. Notably, it could be found that the T_g of PBS component shifted to higher temperatures with increasing PVAc content, and the T_gs of PVAc component in the blends were lower than that of neat PVAc and were nearly unchanged with varying PVAc contents. Such change of T_g with PVAc content indicated that there was an intercompositional interaction between PBS and PVAc in amorphous region, which enhanced the compatibilization in the PBS/PVAc blends [35]. In other words, the blends composed of PBS and PVAc components were partial miscible. Additionally, in a partial miscible blend system, molecular chain interpenetration may take place at the phase interface according to Flory-Huggins parameters, causing components to mutually influence chain mobility at the phase interface [36]. Since the T_g of PVAc was higher than that of PBS, the presence of PBS might promote the chain mobility of PVAc, and the presence of PVAc also might hinder the chain mobility of PBS in the blends because of the partial miscibility between PBS and PVAc in amorphous region. Therefore, a decrease in the T_g of PVAc component and an increase in the T_g of PBS component in the blends were observed.

Figure 1 c illustrates the variations of storage modulus (E') of neat PBS and PVAc and their blends as a function of temperature. Firstly, E' of neat PVAc and PBS dropped sharply in the temperature range of 40 to 50 °C and – 30 to 20 °C, respectively, due to their glass transitions. Secondly, for the blends, when the temperature was below about – 40 °C, the addition of PVAc had no obvious effect on the E' of PBS/PVAc blends due to both components were in the glass state. As the temperature increased to the range of – 40 to 40 °C, which was higher than the T_g of PBS and lower than the T_g of PVAc, the addition of PVAc enhanced the E' of PBS/PVAc blends. The increase in the E' with the PVAc content of PBS/PVAc blends was attributed to the reinforcement of PVAc component caused by its high stiffness under glassy state.

Table 1 T_gs of neat PBS and PVAc and their blends obtained from DMA

PBS/PVAc	100/0	90/10	80/20	70/30	0/100
$T_{g,\ PVAc}$ (°C)	–	43.7	44.9	44.5	49.6
$T_{g,PBS}$ (°C)	− 18.5	− 14.9	− 13.0	− 11.9	–

With temperature continuing to rise above 40 °C, which was higher than the T_g of PVAc, PBS and PVAc were in semi-crystalline state and high elastic state, respectively. The E' of blends dropped to less than that of neat PBS and decreased with an increase in the PVAc content. This was because of the diluting effect of rubbery PVAc segments due to its better mobility at temperature above T_g.

It is well recognized that the morphology of polymer blends is typically used to study the individual polymers miscibility. Miscible blends exhibit single-phase morphology and immiscible blends show phase separation [37]. Figure 2 manifests SEM micrographs of cryo-fractured surfaces for the PBS/PVAc blends after selective etching of PVAc component by acetone solution. The surface of neat PBS was homogeneous and smooth, as shown in Fig. 2 a. In Fig. 2 b–d, the blends showed an obvious phase-separated morphology, which was consistent with the two T_gs measured by DMA. In addition, it was found that the blends showed a well dispersion of PVAc minor phase in the PBS matrix. Figure 3 illustrates the quantitative analyses of dispersed PVAc phase in the blends. As can be seen from Fig. 3, an increase in the PVAc content resulted in an increase in the average particle size (D) of PVAc phase. For example, D of PBS/PVAc blends containing PVAc of 10, 20, and 30 wt% were 0.27, 0.34, and 0.66 μm, respectively. At the same time, the size distribution of PVAc phase also became wider with increasing PVAc content. These results were in line with many immiscible polymer blends [38, 39]. The fine and uniform dispersion and small particle size of PVAc phase suggested a good compatibility in the PBS/PVAc partial miscible blends due to the stronger interaction between PVAc and PBS.

Non-isothermal melt crystallization and melting behaviors

DSC tests were employed to study the effects of PVAc on the non-isothermal melt crystallization and the subsequent melting behaviors of PBS matrix. Figure 4 a shows the DSC cooling scans at a cooling rate of 10 °C min^{-1}. The evaluated parameters obtained from the cooling runs, melt crystallization peak temperatures (T_c), and crystallization enthalpy (ΔH_c) are summarized in Table 2.

Generally speaking, the values of T_c can be used to assess the non-isothermal crystallization nucleation rate [40]. The higher the T_c, the faster the nucleation when polymer crystallizes. T_c of neat PBS was 75.1 °C, while T_c of blend with PVAc content of 10 wt%, 20 wt%, and 30 wt% gradually increased to 79.9 °C, 82.2 °C, and 83.4 °C, respectively. Additionally, the relative crystallinity curves of neat PBS and its blends are shown in Fig. 4 b. Crystallization half-time ($t_{1/2}$), the time for the relative crystallinity to reach 50%, could be obtained from Fig. 4 b and are listed in Table 2. All curves exhibited a sigmoid with respect to time and the $t_{1/2}$ of neat PBS was 1.08 min. It was found that the $t_{1/2}$ of PBS in the blends became shorter with addition of PVAc. These phenomena suggested that the addition of PVAc

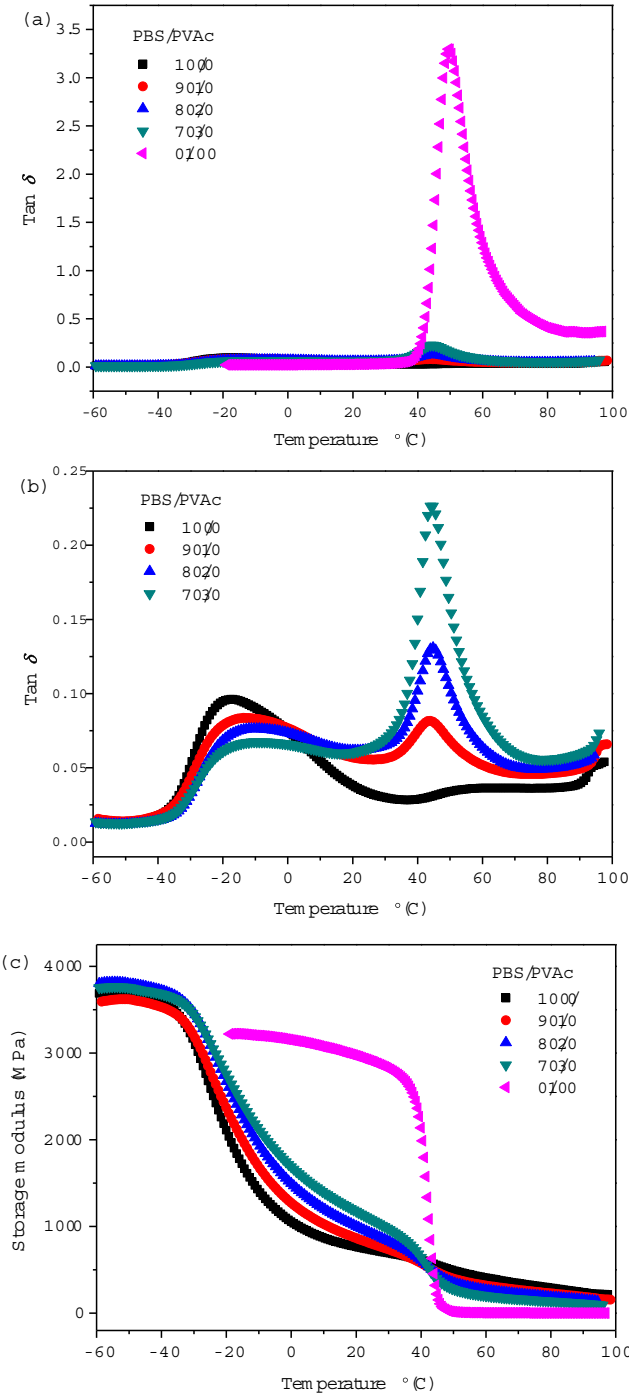

Fig. 1 DMA traces of PBS/PVAc blends with different PVAc contents: **a** tan δ against temperature; **b** magnified image of (**a**) in order to more clearly observe the damping peaks of blends; (**c**) storage modulus (E') against temperature curves

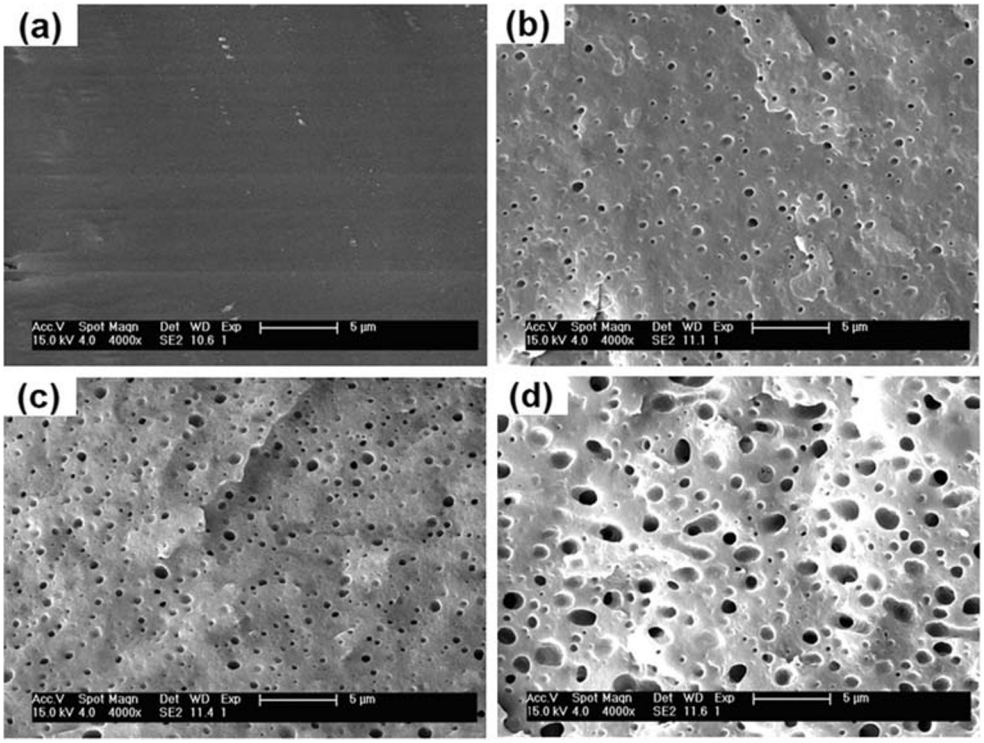

Fig. 2 SEM microphotographs of cryo-fractured surfaces of PBS/PVAc blends after etching in the acetone solution: **a** 100/0, **b** 90/10, **c** 80/20, and **d** 70/30

promoted nucleation and increased crystallization rate of PBS in the blends, and the degree of improvement was obviously affected by the PVAc content. In addition, the non-isothermal crystallization kinetics of neat PBS and PBS/PVAc blends was analyzed by the Avrami equation [41]:

$$1-X_t = \exp(-kt^n) \quad (1)$$

where X_t is relative crystallinity at time t, k is crystallization rate constant, and n is Avrami exponent. Figure 4 c shows the Avrami plots of neat PBS and its blends. The values of k and n were calculated from the intercept and slope of the early linear portion and are listed in Table 2. It was clear that k increased with increasing PVAc content, suggesting that the non-isothermal crystallization rate of blends increased with the increase of PVAc content. Additionally, the n value of neat PBS was 3.5, indicating a heterogeneous nucleation process with three-dimensional growth [42]. The n values of PBS/PVAc blends at a range of 3.3–3.7 were close to that of neat PBS, suggesting that the presence of PVAc did not change the non-isothermal crystallization mechanism of PBS.

In general, for fully immiscible polymer blends, the crystallization process of the matrix phase should not be affected by the minor phase, especially if the matrix polymer crystallizes first. However, when compatibilizers are applied to the immiscible blends, the crystallization behavior and kinetics of the matrix polymer may be affected [36, 43, 44]. For many partially miscible blend systems, it was found that the minor component could retard the crystallization of the matrix component [45–49]. Wu et al. [45] studied the non-isothermal crystallization behavior of partially miscible poly(phenylene sulfide) (PPS)/polycarbonate (PC) blends, and found that the crystallization rate of PPS decreased due to the increasing of viscosity caused by the addition of PC. For the partially miscible six-armed poly(L-lactic acid) (6a-PLLA)/poly(3-hydroxybutyrate-*co*-3-hydroxyvalerate) (PHBV) blends, the crystallization rate of 6a-PLLA decreased with increasing PHBV content because the dilution effect of PHBV exceeded its nucleation effect [46]. Our previous research on polypropylene (PP)/propylene-based random copolymer (PEC) partially miscible blends suggested that the imperfection of PP crystals and the dilution effect of PEC chains resulted in the decrease in the T_c of blends with increasing PEC content [47]. Other partially miscible blends whose crystallization rates were reduced by blending were poly(phenyl acetylene) (PPA)/PCL [48], PBS/PES [28], and PLLA/poly(methyl methacrylate) (PMMA) [49], etc. In this study, it was worth noting that for partially miscible PBS/PVAc blends, the present of PVAc significantly accelerated the non-isothermal melt crystallization rate of PBS matrix. As mentioned above, the good dispersion of PVAc in the PBS matrix could be attributed to the strong interaction between PVAc and PBS, which made PVAc play the main role of heterogeneous nuclei. Its nucleation effect exceeded

the dilution effect. Therefore, the crystallization rates of PBS in the PBS/PVAc blends were accelerated by the heterogeneous nucleation effect of dispersed PVAc component.

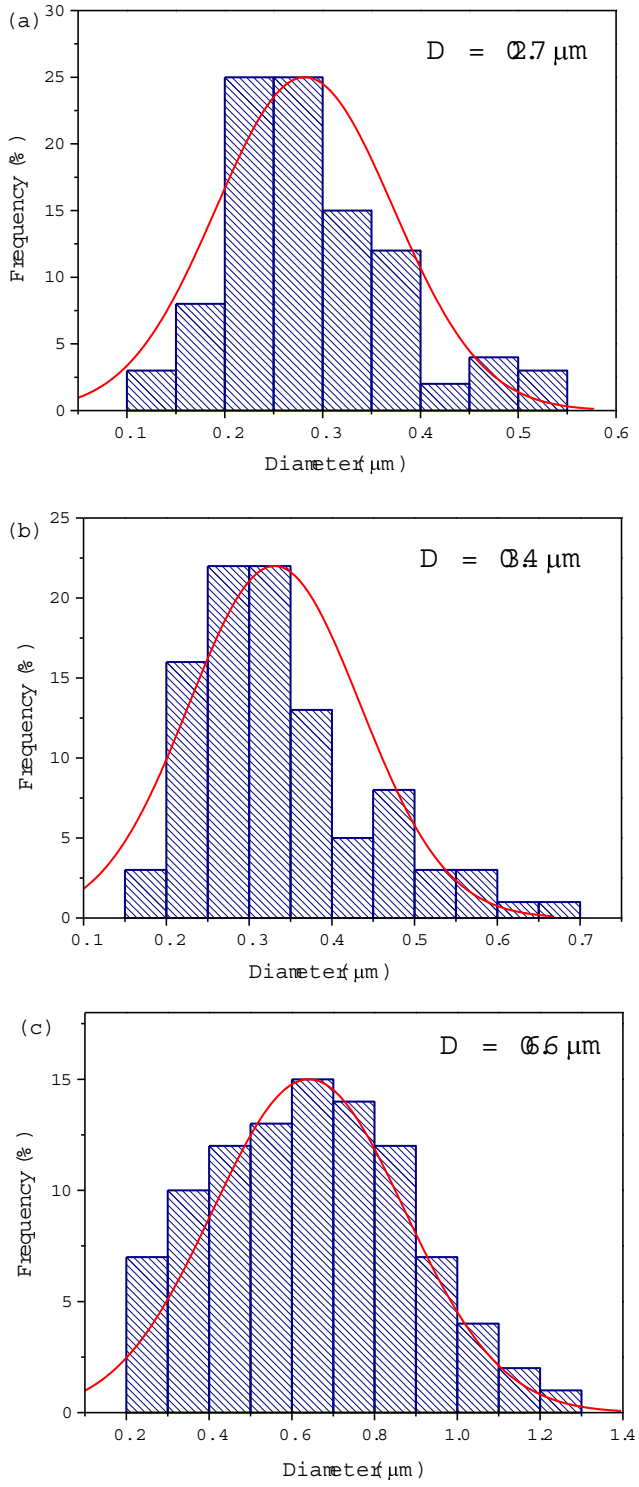

Fig. 3 Quantitative analyses of PVAc phase size distribution based on the SEM micrographs in Fig. 2: **a** 90/10, **b** 80/20, and **c** 70/30. *D* was the average particle diameter

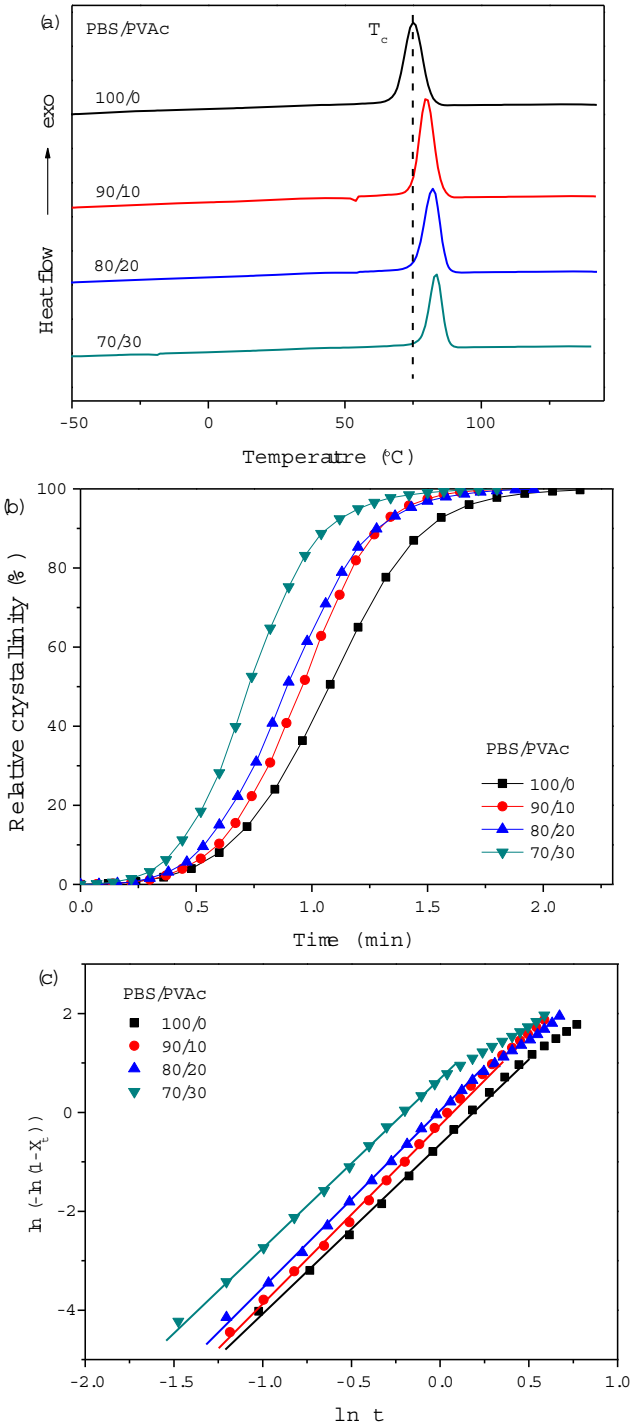

Fig. 4 **a** DSC thermograms of neat PBS and its blends recorded in non-isothermal melt crystallization at a cooling rate of 10 °C min^{-1}, **b** relative crystallinity curves, and **c** Avrami plots

Figure 5 shows the DSC heating curves after non-isothermal melt crystallization of neat PBS and its blends at a heating rate of 10 °C min^{-1}. The thermal parameters including melting endothermic peak (T_m) and melting enthalpy (ΔH_m) are also summarized in Table 2. As observed from Fig. 5, neat PBS showed a T_m at 115.5 °C. The T_ms of blends

Table 2 Non-isothermal melt crystallization, Avrami kinetic, and melting parameters of neat PBS and PBS/PAVc blends

PBS/PVAc	T_c (°C)	$t_{1/2}$ (min)	n	k (min^{-n})	ΔH_c (J/g)	T_m (°C)	ΔH_m (J/g)	X_c (%)
100/0	75.1	1.08	3.5	0.5360	58.5	115.5	57.7	52.3
90/10	79.9	0.95	3.7	0.8322	64.3	113.9	56.2	51.0
80/20	82.2	0.90	3.5	0.9589	65.3	113.6	53.8	48.8
70/30	83.4	0.72	3.3	1.8166	53.4	113.3	45.9	41.6

ΔH_m and ΔH_c are corrected by the content of PBS in the PBS/PVAc blends

were around 2 °C lower than that of neat PBS. From a thermodynamic point of view, the dilution effect of PVAc would lead to a decrease in the T_m of the blends.

The degree of crystallinity (X_c) of blends during crystallization were evaluated by the following relationship and listed in Table 2:

$$X_c(\%) = \frac{\Delta H_m}{\Delta H_m^0 \times \phi} \times 100 \quad (2)$$

where X_c is the degree of crystallinity of PBS phase, ΔH_m is the measured melting enthalpy, φ is the wight content of PBS in the blends, and ΔH_m^0 is the melting enthalpy of PBS crystal with 100% degree of crystallinity, that is 110.3 J g^{-1} [50]. The X_c of neat PBS was 52.3%. The incorporation of PVAc decreased the X_c of PBS. Especially when the PVAc content increased to 30 wt%, the X_c dropped to 41.6%. Consequently, it could be concluded that the present of PVAc increased the crystallization rate of PBS but decreased the X_c of PBS. These findings might be connected with the phase interface in partially miscible blends. The addition of PVAc could accelerate the crystallization rate due to its heterogeneous nuclei caused by the strong interaction between PVAc and PBS, which, in fact, also limited the stacking and arrangement of PBS chains to a large extent, resulting in a decrease in the X_c. Similar phenomena had been observed in other blend systems, such as PBS/cellulose triacetate (CT) and poly(3-hydroxybutyrate-*co*-4-hydroxybutyrate) (P34HB)/PBS [50, 51].

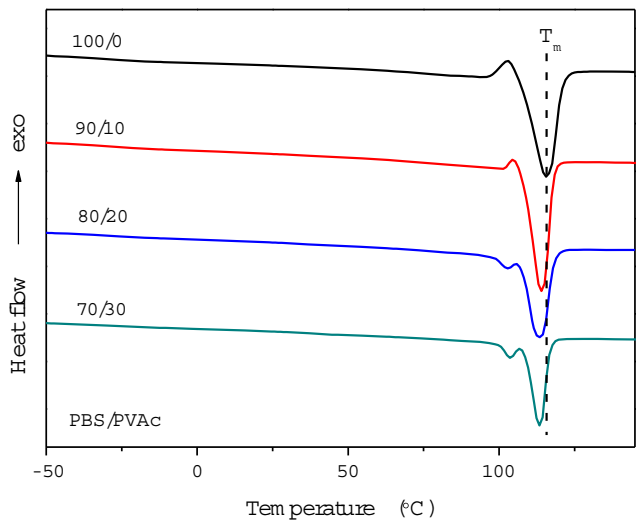

Fig. 5 DSC heating scans after non-isothermal melt crystallization process at a heating rate of 10 °C min^{-1}

Isothermal crystallization behavior and kinetics

Isothermal crystallization behavior and kinetics were studied in order to further explore the effect of PVAc on the

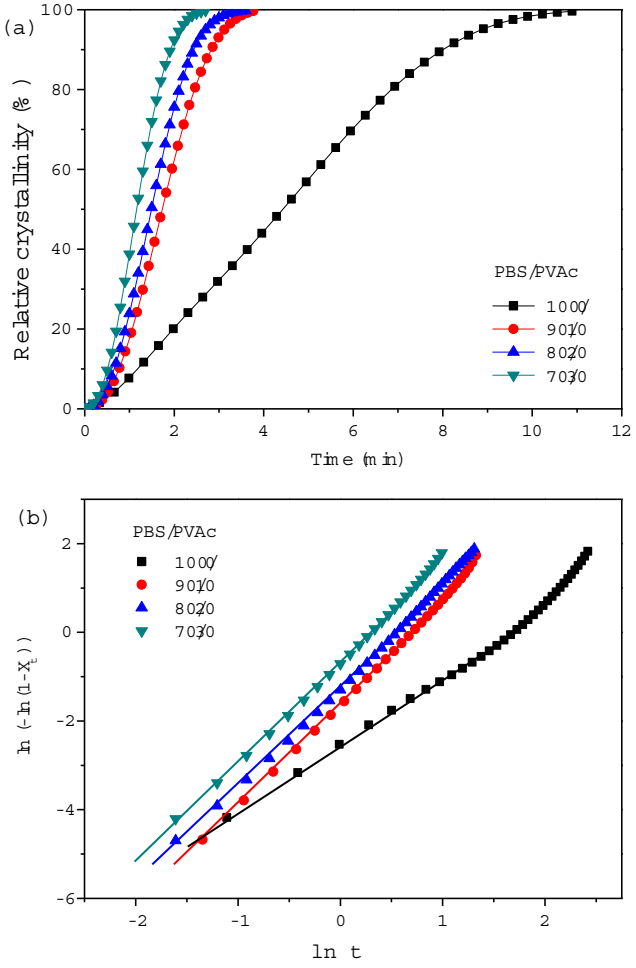

Fig. 6 **a** Variation of relative crystallinity with crystallization time for isothermal melt crystallization of neat PBS and its blends and **b** Avrami plots at 90 °C

Table 3 Kinetics parameters of isothermal melt crystallization of neat PBS and its blends at 90 °C

PBS/PVAc	$t_{1/2}$ (min)	n	k (min^{-n})	R^2
100/0	4.44	1.7	0.0773	0.9911
90/10	1.71	2.4	0.1993	0.9986
80/20	1.48	2.3	0.2952	0.9985
70/30	1.15	2.3	0.5199	0.9983

crystallization process of PBS in the blends. Figure 6 a shows the curves of relative crystallinity versus crystallization time of neat PBS and its blends at crystallization temperatures of 90 °C. Obviously, the crystallization time decreased with increasing PVAc content. The Avrami equation was used to analyze the isothermal crystallization process of PBS/PVAc blend system. Figure 6 b shows the Avrami plots for neat PBS and PBS/PVAc blends at temperatures of 90 °C. The isothermal crystallization kinetic parameters obtained from Fig. 6,

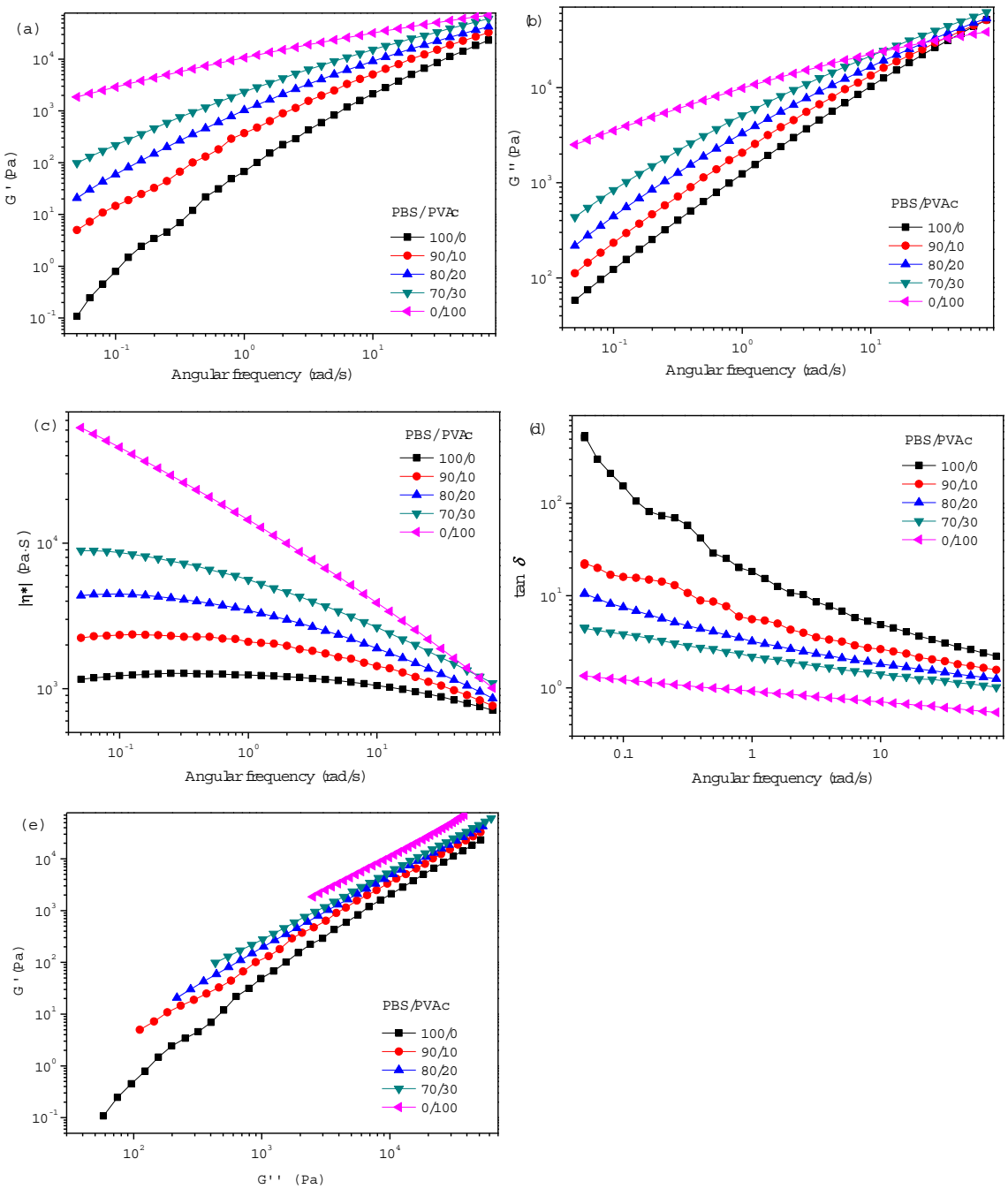

Fig. 7 Plots of **a** storage modulus (G'), **b** loss modulus (G''), **c** complex viscosity ($|\eta^*|$) and **d** loss tangent ($\tan\delta$) as functions of angular frequency, and **e** Han plots of G' vs. G'' for PBS/PVAc blends containing different PVAc concentrations

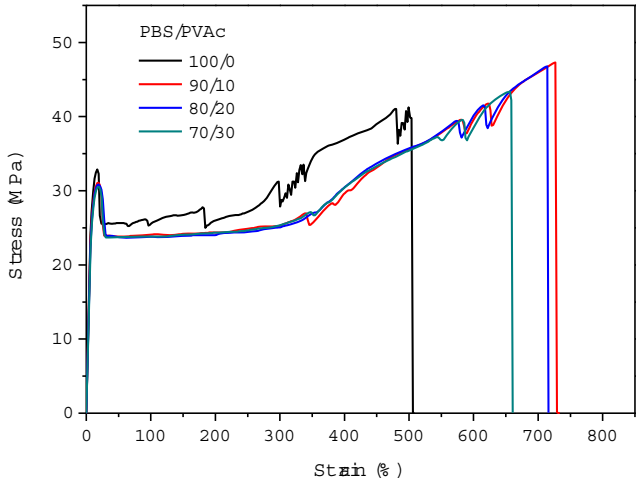

Fig. 8 Stress-strain curves of neat PBS and its blends with various PVAc contents

$t_{1/2}$, n, and k, are listed in Table 3. The $t_{1/2}$ values of blends decreased compared with neat PBS. Moreover, the $t_{1/2}$ values of blends decreased with increasing PVAc content, suggesting that the entire isothermal crystallization rate was increased with an increase in the PVAc loading. This was consistent with the results of non-isothermal crystallization process, and once again illustrated the heterogeneous nucleation of PVAc. The n values varied slightly between 1.7 and 2.4 for neat PBS and PBS/PVAc blends, implying that neat PBS and its blends crystallized through the same mechanism. In other words, the addition of PVAc and the content of PVAc did not change the mechanism of isothermal crystallization of PBS. Furthermore, the crystallization rate constant, k, was found to increase with an increase in the PVAc content. It could be seen that the introduction of PVAc increased both non-isothermal crystallization and isothermal crystallization rate of PBS in the blends due to heterogeneous nucleation of PVAc, but it had almost no effect on the crystallization mechanism.

Rheological properties

Rheological properties can well characterize the structure and interaction of polymers because of their sensitivity to rheological properties. To check the effect of PVAc on the rheological properties of the blends, oscillatory shear rheological tests were conducted at 150 °C. The influence of PVAc content on the storage modulus (G'), loss modulus (G''), complex viscosity ($|\eta^*|$), loss tangent (tan δ), and Han plots of PBS in the blends is shown in Fig. 7.

It was seen that neat PBS demonstrated an obvious liquid-like behavior at low-frequency zone with logarithmic G' and G'' versus logarithmic angular frequency showed a good linear relationship of $G' \propto 1.40$ and $G'' \propto 0.79$, respectively. Neat PVAc showed a significant pseudo-solid-like behavior, due to the slopes of logarithmic G' and G'' versus logarithmic angular frequency were 0.28 and 0.42, respectively [52]. This was mainly because of the high viscosity of PVAc in the melt state. For the blends, on the one hand, the slopes of G' curves at low-frequency zone decreased with increasing PVAc content, on the other hand, both G' and G'' increased monotonically within the test frequency range with an increase in the PVAc content. These results indicated that PVAc possessing high viscosity in the melt could improve the melt strength of PBS matrix.

It could be observed from Fig. 7 c that the $|\eta^*|$ of neat PBS showed a Newtonian liquid behavior; in contrast, the $|\eta^*|$ of neat PVAc exhibited non-Newtonian shear-thinning behavior. In terms of blends, the $|\eta^*|$ gradually increased with increasing PVAc content, and Newtonian plateau appeared in the low-frequency region, and the non-Newtonian shear thinning in the high-frequency region. At the same time, for the blends with a higher concentration of PVAc, the Newtonian plateau in the low-frequency region narrowed even disappeared. It was due to the fact that the measurement frequency range was not low enough for the blends with higher content of PVAc. Moreover, the loss tangent ($\tan \delta = G''/G'$), the ratio of dissipated energy to stored energy, is considered to be a more sensitive parameter to the relaxation variation of polymer than G' or G'' [52]. Figure 7 d illustrates the loss tangent of all samples as a function of frequency. The tan δ of neat PBS decreased with increasing frequency, which was consistent with the behavior of typical viscoelastic liquids. As the PVAc concentration was increased, tan δ of the blends gradually decreased, indicating the larger increasing ratio of storage modulus than the increasing ratio of viscosity. Han plots of $G' \sim G''$ [53] showed in Fig. 7 e can be used to determine the miscibility of

Table 4 Mechanical properties of neat PBS and PBS/PAVc blends tested at room temperature

PBS/PVAc	Young's modulus (MPa)	Yield strength (MPa)	Breaking strength (MPa)	Elongation at break (%)
100/0	345 ± 13	32.7 ± 1.6	40.8 ± 2.1	505 ± 19
90/10	357 ± 9	30.7 ± 0.8	47.2 ± 1.5	724 ± 22
80/20	362 ± 11	30.5 ± 1.2	46.6 ± 1.2	701 ± 21
70/30	372 ± 15	30.3 ± 0.6	43.3 ± 1.9	655 ± 18

the blends. If the slopes of the Han curves of the blends are similar in the low-frequency region, the compatibility between the components is good; otherwise, they are not miscible [54]. It can be seen from the Fig. 7 e that as the content of PVAc increased, the slopes of the Han curves of PBS/PVAc blends in the low-frequency region did not change much, indicating a good miscibility between PBS and PVAc, which was consistent with the DSC results. In short, the addition of PVAc significantly enhanced the rheological properties of PBS, which was helpful to improve the relative difficulty of processability for PBS caused by its low viscosity in the melt, making major thermoplastic processing methods possible, such as injection molding, blow molding, extrusion molding, and compression molding.

Tensile mechanical property

Figure 8 shows the tensile stress-strain curves of neat PBS and PBS/PVAc blends and Table 4 lists the relevant mechanical properties. Neat PBS was a soft polymer, exhibiting modulus and breaking strength of 345 and 40.8 MPa, respectively, as well as a high elongation at break of 505%. Moreover, neat PBS showed a distinct yield point with yield strength of 32.7 MPa, followed by a neck growth, strain hardening, and finally fracture. All PBS/PVAc blends displayed clear yielding, more stable neck growth, and greater stress hardening, compared to neat PBS. Therefore, the elongation at break of blends drastically increased with increasing PVAc content. Surprisingly, it was found the breaking strength and modulus of blends were also higher than those of neat PBS. Especially for the blend constituting 10 wt% PVAc, the modulus, breaking strength, and elongation at break arose up to 357 MPa, 47.2 MPa, and 724%, respectively, which increased by 3.5%, 15.7%, and 43.4% compared to pure PBS. In other words, the incorporation of PVAc played a role in strengthening and toughening PBS at the same time. Hemsri et al. [55] prepared PBS/acrylonitrile butadiene rubber (NBR) blends by using dicumyl peroxide (DCP) as a vulcanizing agent, and found that although the elongation at break of blend with 30 wt% NBR increased by about 1300%, the tensile strength reduced from 44.8 to 29.5 MPa. For PBS/thermoplastic starch (TPS) blends with glycerol as plasticizers, both the tensile strength and elongation at break decreased with increasing TPS content [56]. Ostrowska et al. [57] reported that the elongation at break of PBS/PLA blend with 30 wt% PLA reduced by 17% and tensile strength reduced by 13%. In our study, the unexpected combination of enhanced toughness and strength was obtained by incorporation of PVAc. The modulus of the blends was higher than that of pure PBS due to a relatively high hardness of PVAc at room temperature caused by its higher T_g than PBS, and a strong interaction between PBS and PVAc chains as DMA result aforementioned. Moreover, from the above DSC results, it could be seen that the addition of PVAc reduced the X_c of PBS. Therefore, during stretching, the more amorphous region of PBS matrix in the blends could be easily oriented and hardened to a greater extent, resulting in an increase in breaking strength and elongation at break.

Conclusions

In this study, PBS blends incorporating PVAc were prepared by using melt mixing at various PVAc loading. Based on DMA measurements, it was found that the blends were partial miscibility due to the strong interaction between PBS phase and PVAc phase. The effect of PVAc on the storage modulus of blends was different in various temperature ranges, depending on the physical states of PVAc and PBS. On the basis of morphological observations, it demonstrated that the blends exhibited a well dispersion of PVAc minor phase in the PBS matrix. The size of PVAc phase increased with increasing PVAc content. The crystallization behavior analysis suggested that the introduction of PVAc accelerated both non-isothermal crystallization and isothermal crystallization rates of PBS in the blends due to heterogeneous nucleation of PVAc, but it had almost no effect on the crystallization mechanism. However, the present of PVAc decreased the X_c of PBS. Rheological properties tests showed that the storage modulus, loss modulus, and complex viscosity of PBS/PVAc blends were increased with the increase in the PVAc content due to the higher viscosity of PVAc, which was beneficial to the thermoplastic processing of PBS. Unexpectedly, the incorporation of PVAc simultaneously improved the elongation at break, modulus, and breaking strength of blends.

Funding This work is financially supported by the Chinese Academy of science and technology service network planning (KFJ-STS-QYZD-140), a program of Zhongshan Science and Technology Bureau (2017A1037), Innovation team project of Beijing Institute of Science and Technology (IG201703N), and "13th five-year" Science and Technology Research Program of the Education Department of Jilin Province (JJKH20190862KJ).

Compliance with ethical standards

Conflict of interest The authors declare that they have no conflict of interest.

References

1. Pawar SP, Misra A, Bose S, Chatterjee K, Mittal V (2015) Enzymatically degradable and flexible bio-nanocomposites derived from PHBV and PBAT blend: assessing thermal, morphological, mechanical, and biodegradation properties. Colloid Polym Sci 293: 2921–2930
2. Liu G, Zheng L, Zhang X, Li C, Wang D (2014) Critical stress for crystal transition in poly(butylene succinate)-based crystalline-amorphous multiblock copolymers. Macromolecules 47:7533–7539
3. Du X, Wang Y, Huang W, Yang J, Wang Y (2015) Rheology and non-isothermal crystallization behaviors of poly(butylene succinate)/graphene oxide composites. Colloid Polym Sci 293:389–400
4. Shi K, Liu Y, Hu X, Su T, Li P, Wang Z (2018) Preparation, characterization, and biodegradation of poly(butylene succinate)/cellulose triacetate blends. Int J Biol Macromol 114:373–380
5. Wang P, Tian Y, Wang G, Xu Y, Yang B, Lu B, Zhang W, Ji J (2015) Surface interaction induced transcrystallization in biodegradable poly(butylene succinate)-fibre composites. Colloid Polym Sci 293:2701–2707
6. Chen C, Peng JS, Chen M, Lu HY, Tsai CJ, Yang CS (2010) Synthesis and characterization of poly(butylene succinate) and its copolyesters containing minor amounts of propylene succinate. Colloid Polym Sci 288:731–738
7. Han SO, Lee SM, Park WH, Cho D (2006) Mechanical and thermal properties of waste silk fiber-reinforced poly(butylene succinate) biocomposites. J Appl Polym Sci 100:4972–4980
8. The DT, Yoshii F, Nagasawa N, Kume T (2003) Synthesis of poly(butylene succinate)/glass fiber composite by irradiation and its biodegradability. J Appl Polym Sci 94:2122–2127
9. Liang J, Ding C, Wei Z, Sang L, Song P, Chen G, Chang Y, Xu J, Zhang W (2015) Mechanical, morphology, and thermal properties of carbon fiber reinforced poly(butylene succinate) composites. Polym Compos 36:1335–1345
10. Someya Y, Nakazato T, Teramoto N, Shibata M (2004) Thermal and mechanical properties of poly(butylene succinate) nanocomposites with various organo-modified montmorillonites. J Appl Polym Sci 91:1463–1475
11. Wang G, Guo B, Xu J, Li R (2011) Rheology, crystallization behaviors, and thermal stabilities of poly(butylene succinate)/pristine multiwalled carbon nanotube composites obtained by melt compounding. J Appl Polym Sci 121:59–67
12. Liang Z, Pan P, Zhu B, Dong T, Inoue Y (2010) Mechanical and thermal properties of poly(butylene succinate)/plant fiber biodegradable composite. J Appl Polym Sci 115:3559–3567
13. Ohkita T, Lee S-H (2010) Crystallization behavior of poly(butylene succinate)/corn starch biodegradable composite. J Appl Polym Sci 97:1107–1114
14. Huang J, Lu X, Zhang N, Yang L, Qu J (2014) Study on the properties of nano-TiO_2/polybutylene succinate composites prepared by vane extruder. Polym Compos 35:53–59
15. Zakharova E, Lavilla C, Alla A, Martínez de Ilarduya A, Muñoz-Guerra S (2014) Modification of properties of poly(butylene succinate) by copolymerization with tartaric acid-based monomers. Eur Polym J 61:263–273
16. Charlon S, Marais S, Dargent E, Soulestin J, Sclavonsf M, Follaina N (2015) Structure–barrier property relationship of biodegradable poly(butylene succinate) and poly[(butylene succinate)-*co*-(butylene adipate)] nanocomposites: influence of the rigid amorphous fraction. Phys Chem Chem Phys 17:29918–29934
17. Gan Z, Abe H, Kurokawa H, Doi Y (2001) Solid-state microstructures, thermal properties, and crystallization of biodegradable poly(butylene succinate) (PBS) and its copolyesters. Biomacromolecules 2:605–613
18. Gigli M, Lotti N, Gazzano M, Finelli L, Munari A (2012) Novel eco-friendly random copolyesters of poly(butylene succinate) containing ether-linkages. React Funct Polym 72:303–310
19. Li S, Wu F, Yang Y, Wang Y, Zeng J (2015) Synthesis, characterization and isothermal crystallization behavior of poly(butylene succinate)-b-poly(diethylene glycol succinate) multiblock copolymers. Polym Adv Technol 26:1003–1013
20. Zeng J, Li Y, Zhu Q, Yang K, Wang X, Wang Y (2009) A novel biodegradable multiblock poly(ester urethane) containing poly(L-lactic acid) and poly(butylene succinate) blocks. Polymer 50:1178–1186
21. Zhu Q, He Y, Zeng J, Huang Q, Wang Y (2011) Synthesis and characterization of a novel multiblock copolyester containing poly(-ethylene succinate) and poly(butylene succinate). Mater Chem Phys 130:943–949
22. Lee S-l YS-C, Lee Y-S (2001) Degradable polyurethanes containing poly(butylene succinate) and poly(ethylene glycol). Polym Degrad Stab 72:81–87
23. Huang C, Jiao L, Zhang J, Zeng J, Yang K, Wang Y (2012) Poly(butylene succinate)-poly(ethylene glycol) multiblock copolymer: synthesis, structure, properties and shape memory performance. Poly Chem-UR 3:800–808
24. D'Ambrosio R, Michell RM, Mincheva R, Hernandez R, Mijangos C, Dubois P, MHYPERLIJ (2017) Crystallization and stereocomplexation of PLA-mb-PBS multi-block copolymers. Polymers 10:8
25. Zhang Y, Wang X, Wang Y, Yang K, Li J (2005) A novel biodegradable polyester from chain-extension of poly(*p*-dioxanone) with poly(butylene succinate). Polym Degrad Stab 88:294–299
26. Wu D, Yuan L, Laredo E, Zhang M, Zhou W (2012) Interfacial properties, viscoelasticity, and thermal behaviors of poly(butylene succinate)/polylactide blend. Ind Eng Chem Res 51:2290–2298
27. Wang H, Gan Z, Schultz JM, Yan S (2008) A morphological study of poly(butylene succinate)/poly(butylene adipate) blends with different blend ratios and crystallization processes. Polymer 49:2342–2353
28. He Y, Zeng J, Li S, Wang Y (2012) Crystallization behavior of partially miscible biodegradable poly(butylene succinate)/poly(ethylene succinate) blends. Thermochim Acta 529:80–86
29. Sivalingam G, Karthik R, Madras G (2004) Blends of poly(ε-caprolactone) and poly(vinyl acetate): mechanical properties and thermal degradation. Polym Degrad Stab 84:345–351
30. Gajria AM, Davé V, Gross RA, McCarthy SP (1996) Miscibility and biodegradability of blends of poly(lactic acid) and poly(vinyl acetate). Polymer 37:437–444
31. Huang T, Yang J, Zhang N, Zhang J, Wang Y (2018) Crystallization of poly(L-lactide) in the miscible poly(L-lactide)/poly(vinyl acetate) blend induced by carbon nanotubes. Polym Bull 75:2641–2655
32. An Y, Li L, Dong L, MO Z, Feng Z (1999) Nonisothermal crystallization and melting behavior of poly(β-hydroxybutyrate)-poly(vinyl-acetate) blends. J Polym Sci Polym Phys 37:443–450
33. Shafee EE (2001) Investigation of the phase structure of poly(3-hydroxybutyrate) /poly(vinyl acetate) blends by dielectric relaxation spectroscopy. Eur Polym J 37:451–458
34. Yin J, Alfonso GG, Turturro A, Pedemonte E (1993) Thermodynamics of poly(ethylene oxide)–poly(vinyl acetate) blends. Polymer 34:1465–1470
35. Juliana AL, Felisberti MI (2006) Poly(hydroxybutyrate) and epichlorohydrin elastomers blends: phase behavior and morphology. Eur Polym J 42:602–614
36. Kajiyama T, Tanaka K, Takahara A (1997) Surface molecular motion of the monodisperse polystyrene films. Macromolecules 30: 280–285

37. Bauer KN, Tee HT, Lieberwirth I, Wurm FR (2016) In-chain poly(phosphonate)s via acyclic diene metathesis polycondensation. Macromolecules 49:3761–3768
38. Han L, Han C, Zhang H, Chen S, Dong L (2012) Morphology and properties of biodegradable and biosourced polylactide blends with poly(3-hydroxybutyrate-*co*- 4-hydroxybutyrate). Polym Compos 33:850–859
39. Li Y, Li Y, Han C, Yu Y, Xiao L (2019) Morphology and properties in the binary blends of polypropylene and propylene-ethylene random copolymers. Polym Bull 76:2851–2866
40. Wei XF, Bao RY, Cao ZQ, Zhang LQ, Liu ZY, Yang W, Xue B, Yang M (2014) Greatly accelerated crystallization of poly(lactic acid): cooperative effect of stereocomplex crystallites and polyethylene glycol. Colloid Polym Sci 92:163–172
41. Avrami M (1941) Granulation, phase change, and microstructure kinetics of phase change. III. J Chem Phys 9:177–184
42. Tsuji H, Tezuka Y (2004) Stereocomplex formation between enantiomeric poly(lactic acid)s. 12. Spherulite growth of low-molecular-weight poly (lactic acid)s from the melt. Biomacromolecules 5: 118181w-m
43. Shibata M, Teramoto N, Inoue Y (2007) Mechanical properties, morphologies, and crystallization behavior of plasticized poly(L-lactide)/poly(butylene succinate-*co*- L-lactate) blends. Polymer 48:2768–2777
44. Zhang C, Zhai T, Turng LS, Dan Y (2015) The morphological, mechanical, and crystallization behavior of polylactide/polycaprolactone blends compatibilized by L-lactide/caprolactone copolymer. Ind Eng Chem Res 54:9505–9511
45. Wu D, Zhang Y, Zhang M, Wu L (2007) Morphology, nonisothermal crystallization behavior, and kinetics of poly(phenylene sulfide)/polycarbonate blend. J Appl Polym Sci 105:739–748
46. Jiang N, Abe H (2015) Crystallization and melting behavior of partially miscible six-armed poly(L-lactic acid)/poly(3-hydroxybutyrate-*co*-3-hydroxyvalerate) blends. J Appl Polym Sci 42548
47. Li Y, Li Y, Han C, Yu Y, Xiao L (2019) Morphology and properties in the binary blends of polypropylene and propylene-ethylene random copolymers. Polym Bull 76:2851–2866
48. Chen HL, Liaw DJ, Liaw BY, Shih CL, Tsai JS (1998) Compatibility and crystallization studies on poly(phenyl acetylene)/polycaprolactone blend. Polym J 30:874–878
49. Zhang G, Zhang J, Wang S, Shen D (2003) Miscibility and phase structure of binary blends of polylactide and poly(methyl methacrylate). J Polym Sci Polym Phys 41:23–30
50. Shi K, Liu Y, Hu X, Su T, Li P, Wang Z (2018) Preparation, characterization, and biodegradation of poly(butylene succinate)/cellulose triacetate blends. Int J Biol Macromol 114:373–380
51. Zhu W, Wang X, Chen X, Xu K (2009) Miscibility, crystallization, and mechanical properties of poly(3-hydroxybutyrate-*co*-4-hydroxybutyrate)/poly(butylene succinate) blends. J Appl Polym Sci 114:3923–3931
52. Shenoy AV (1999) Rheology of filled polymer systems. Springer, Netherlands, p 90
53. Han CD, Ki JK (1993) On the use of time-temperature superposition in multicomponent/multiphase polymer systems. Polymer 34: 2533–2539
54. Jafari SH, Hesabi MN, Khonakdar HA, Asl-Rahimi M (2011) Correlation of rheology and morphology and estimation of interfacial tension of immiscible COC/EVA blends. J Polym Res 18:821–831
55. Hemsri S, Thongpin C, Moradokpermpoon N, Niramon P, Suppaso M (2015) Mechanical properties and thermal stability of poly(butylene succinate)/acrylonitrile butadiene rubber blend. Macromol Symp 354:145–154
56. Yun IS, Hwang SW, Shim JK, Seo KH (2016) A study on the thermal and mechanical properties of poly (butylene succinate)/thermoplastic starch binary blends. Int J of Pr Eng Man-GT 3: 289–296
57. Ostrowska J, Sadurski W, Paluch M, Tyński P, Bogusz J (2019) The effect of poly(butylene succinate) content on the structure, thermal and mechanical properties of its blends with polylactide. Polym Int 68:1271–1279